

## Supporting Information

### ***In situ fabrication of fluorine-modified acrylate-based gel polymer electrolytes for lithium-metal batteries***

Kun Yang<sup>1</sup>, Zhichuan Shen<sup>1</sup>, Junqiao Huang<sup>1</sup>, Jiawei Zhong<sup>1</sup>, Yuhan Lin<sup>1</sup>, Junli Zhu<sup>1</sup>,

Jiashun Chen<sup>1</sup>, Yating Wang<sup>1</sup>, Tangtang Xie<sup>2,3</sup>, Jie Li<sup>2\*</sup>, Zhicong Shi<sup>1,4\*</sup>

<sup>1</sup> Institute of Batteries, School of Materials and Energy, Guangdong University of Technology, Guangzhou, 510006, China

<sup>2</sup> Department of Energy, Politecnico di Milano, Via Lambruschini, 4, Milano, 20156, Italy

<sup>3</sup> The Testing and Technology Center for Industrial Products, Shenzhen Customs, Shenzhen, Guangdong, 518067, China

<sup>4</sup> Key Laboratory of Advanced Energy Materials Chemistry (Ministry of Education), Nankai University, Tianjin, 300071, China



**Fig. S1.** Digital images of GPEs before and after thermal polymerization.

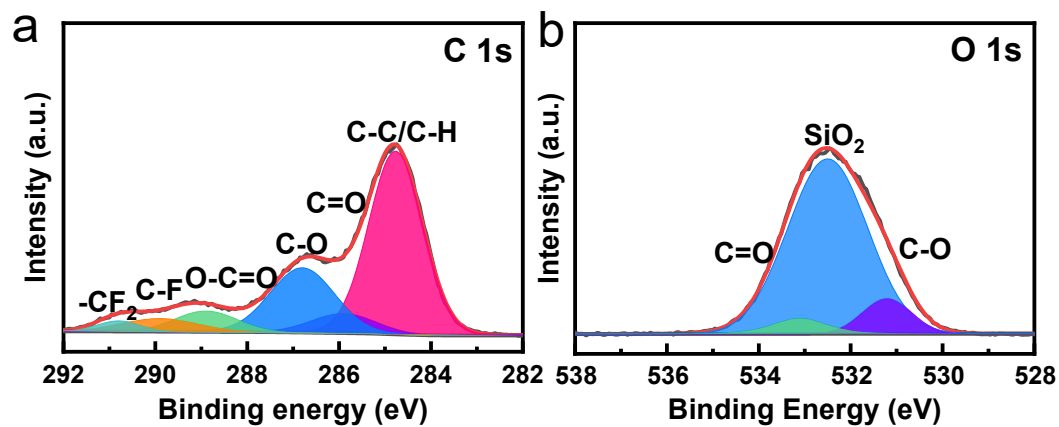


**Fig. S2.** XPS spectra on (a) C 1s and (b) O 1s of 0.4TGD-0.4TFM-TCGG-SiO<sub>2</sub>NF.

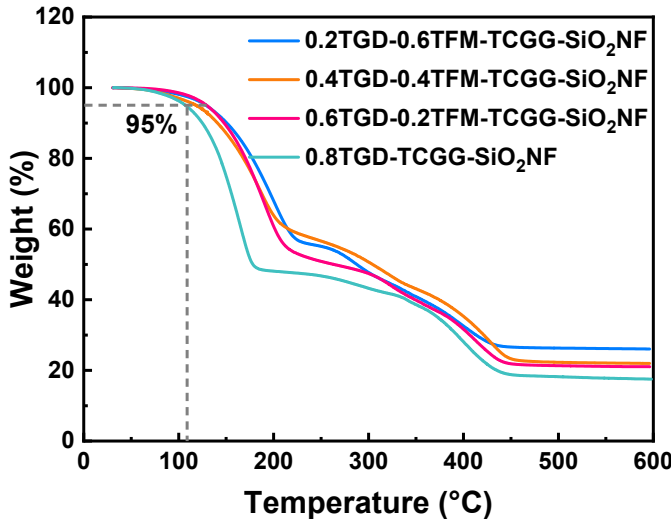


**Fig. S3.** TG curves of 0.8TGD-TCGG-SiO<sub>2</sub>NF, 0.6TGD-0.2TFM-TCGG-SiO<sub>2</sub>NF, 0.4TGD-0.4TFM-TCGG-SiO<sub>2</sub>NF, and 0.2TGD-0.6TFM-TCGG-SiO<sub>2</sub>NF.

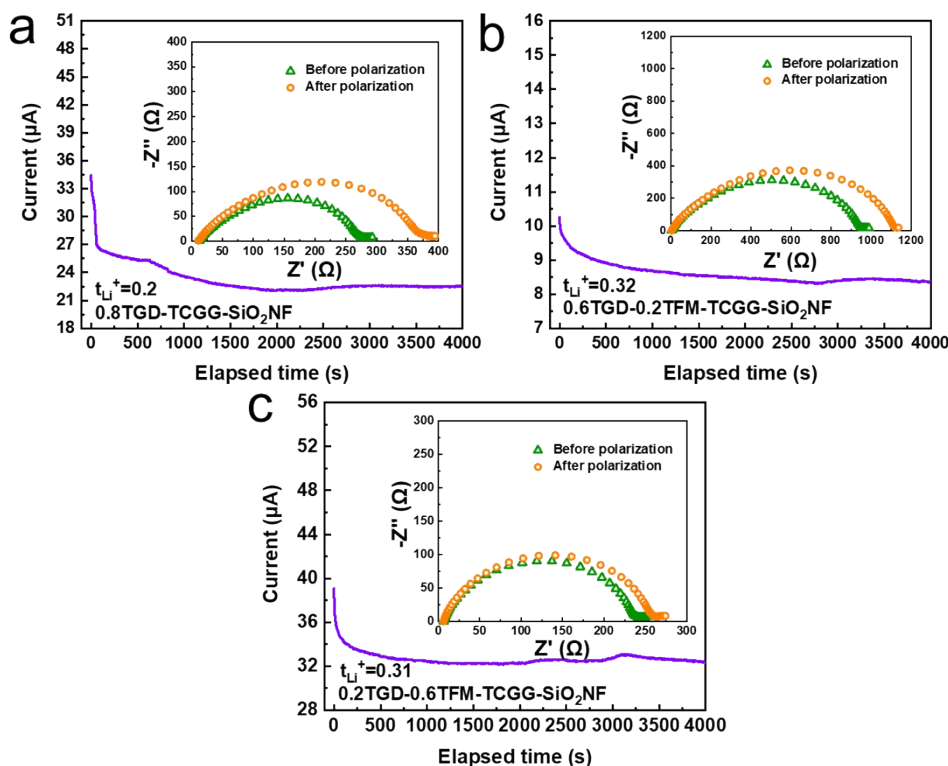


**Fig. S4.** Current and EIS curves of (a) 0.8TGD-TCGG-SiO<sub>2</sub>NF, (b) 0.6TGD-0.2TFM-TCGG-SiO<sub>2</sub>NF, and (c) 0.2TGD-0.6TFM-TCGG-SiO<sub>2</sub>NF before and after polarization at 25 °C.

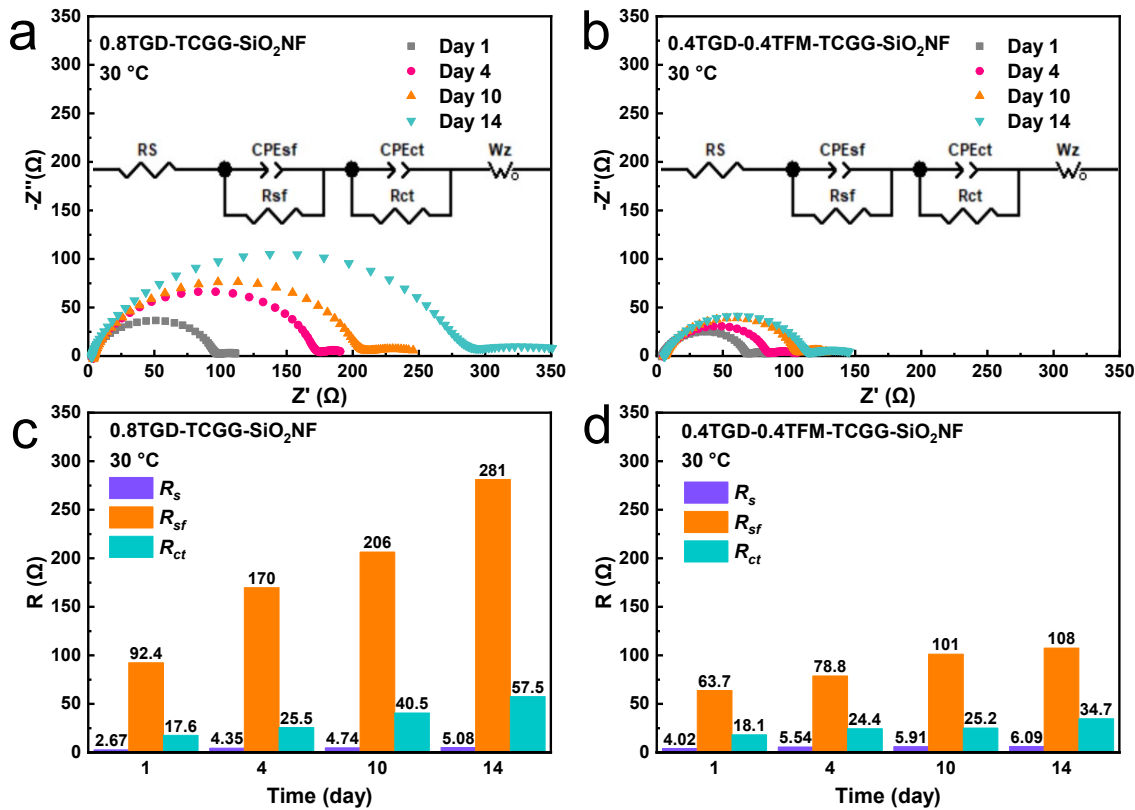


**Fig. S5.** EIS curves and fitting results of Li|0.8TGD-TCGG-SiO<sub>2</sub>NF|Li and Li|0.4TGD-0.4TFM-TCGG-SiO<sub>2</sub>NF|Li cells at 30 °C.

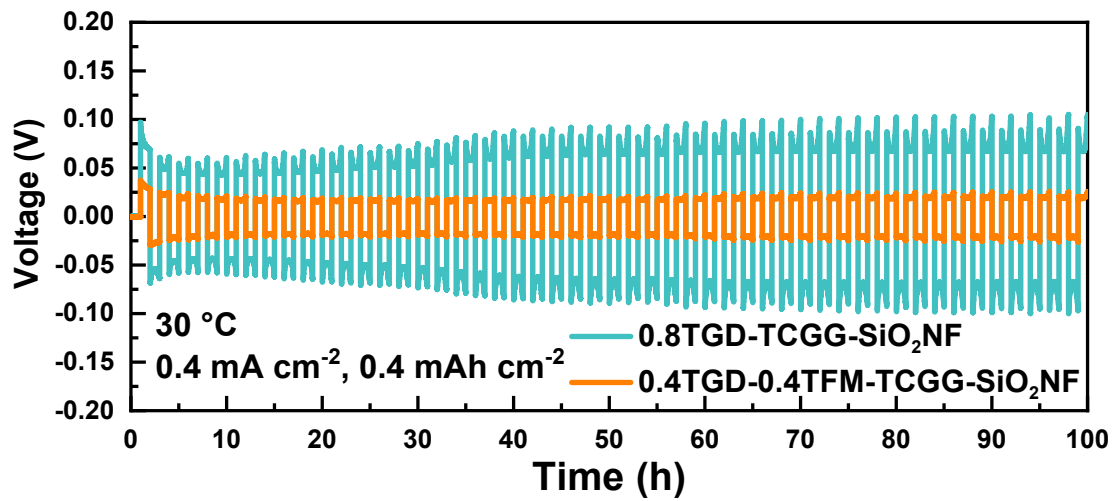


**Fig. S6.** Galvanostatic cycling profiles of Li|0.8TGD-TCGG-SiO<sub>2</sub>NF|Li and Li|0.4TGD-0.4TFM-TCGG-SiO<sub>2</sub>NF|Li cells at the current densities of 0.4 mA cm<sup>-2</sup> with a restricted specific capacity of 0.4 mAh cm<sup>-2</sup> at 30 °C.

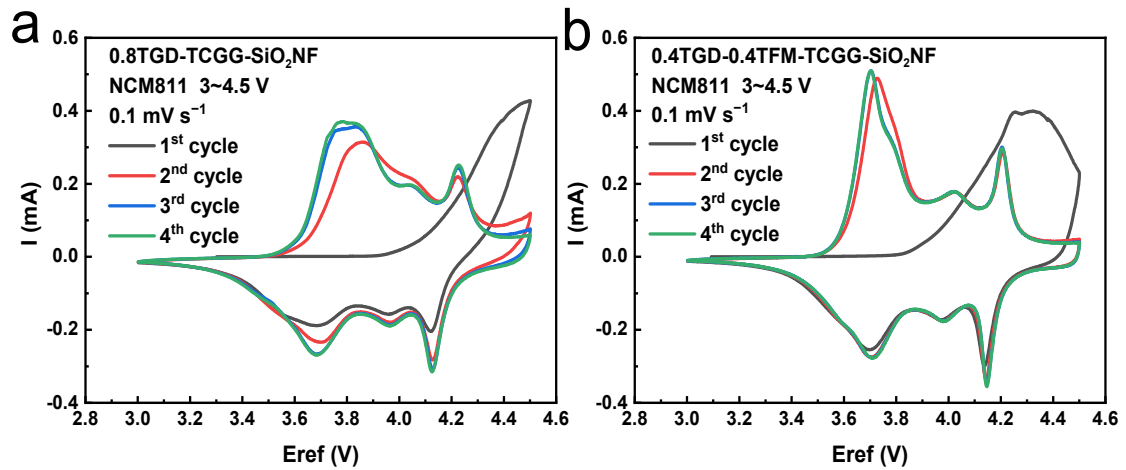


**Fig. S7.** CV curves of (a) NCM811|0.8TGD-TCGG-SiO<sub>2</sub>NF|Li and (b) NCM811|0.4TGD-0.4TFM-TCGG-SiO<sub>2</sub>NF|Li batteries at 3.0 ~ 4.5 V with a scan rate of 0.1 mV s<sup>-1</sup> at 30 °C.

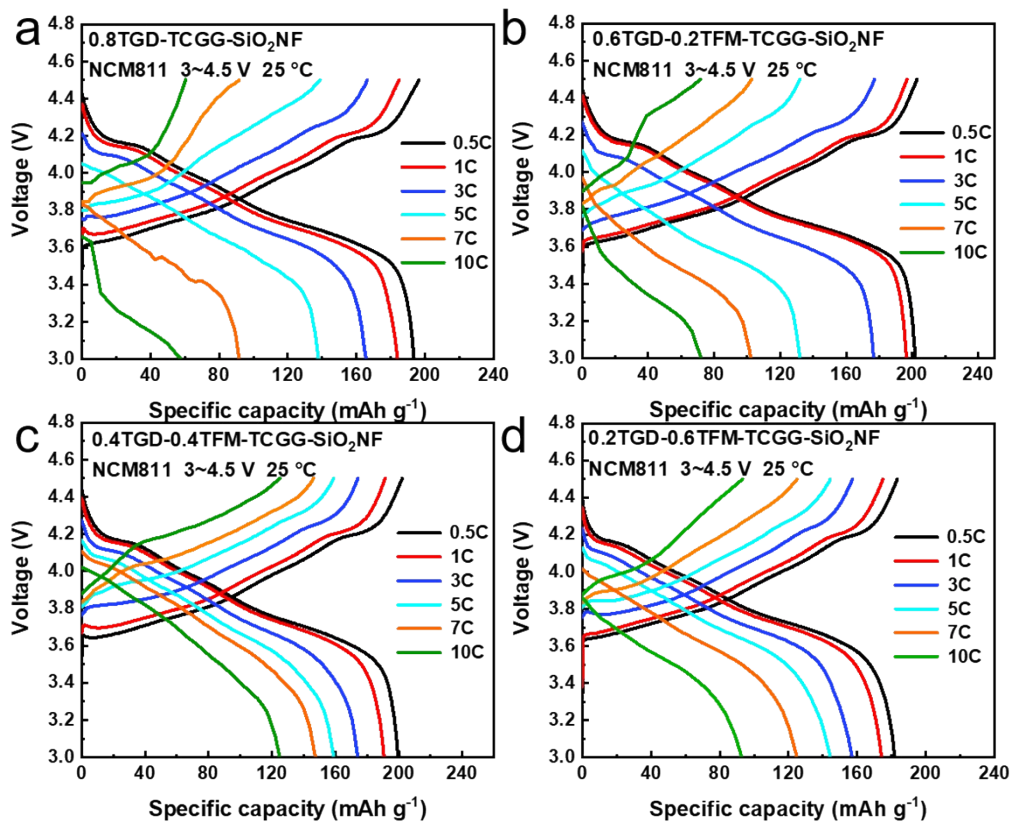


**Fig. S8.** Voltage profiles of (a) NCM811|0.8TGD-TCGG-SiO<sub>2</sub>NF|Li, (b) NCM811|0.6TGD-0.2TFM-TCGG-SiO<sub>2</sub>NF|Li, (c) NCM811|0.4TGD-0.4TFM-

TCGG-SiO<sub>2</sub>NF|Li, and (d) NCM811|0.2TGD-0.6TFM-TCGG-SiO<sub>2</sub>NF|Li batteries at various C-rate.

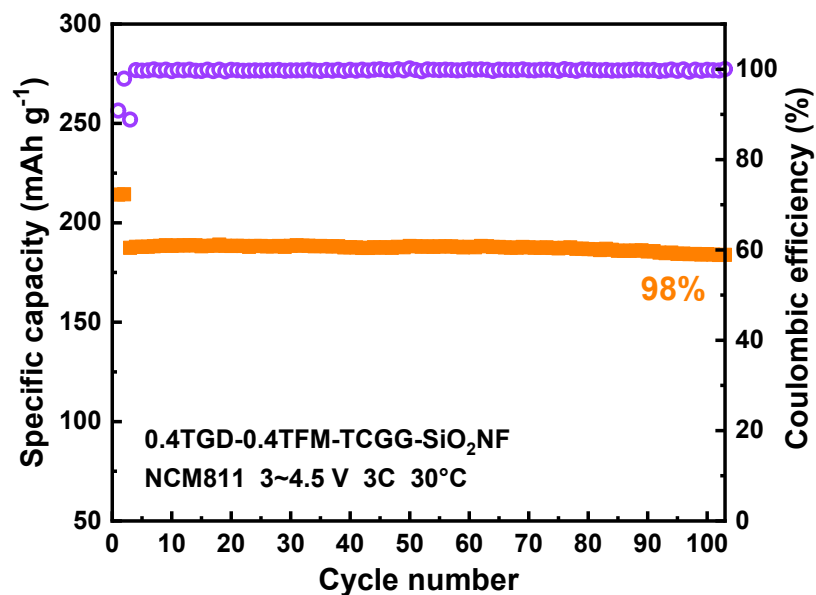


**Fig. S9.** Cycling performance of NCM811|0.4TGD-0.4TFM-TCGG-SiO<sub>2</sub>NF|Li battery at 3C.

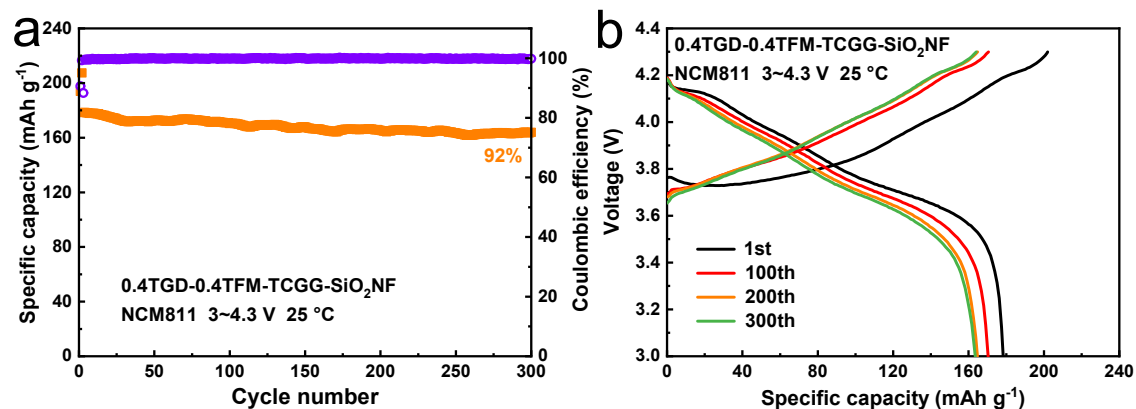


**Fig. S10.** (a) Cycling performance and (b) voltage profiles of NCM811|0.4TGD-0.4TFM-TCGG-SiO<sub>2</sub>NF|Li battery at 2C.

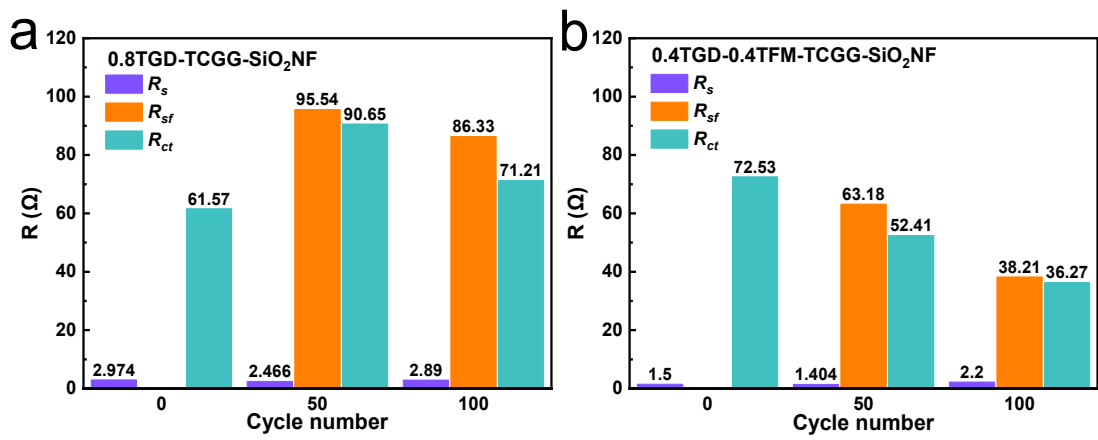


**Fig. S11.**  $R_s$ ,  $R_{sf}$ , and  $R_{ct}$  variation of NCM811|0.8TGD-TCGG-SiO<sub>2</sub>NF|Li and NCM811|0.4TGD-0.4TFM-TCGG-SiO<sub>2</sub>NF|Li batteries.

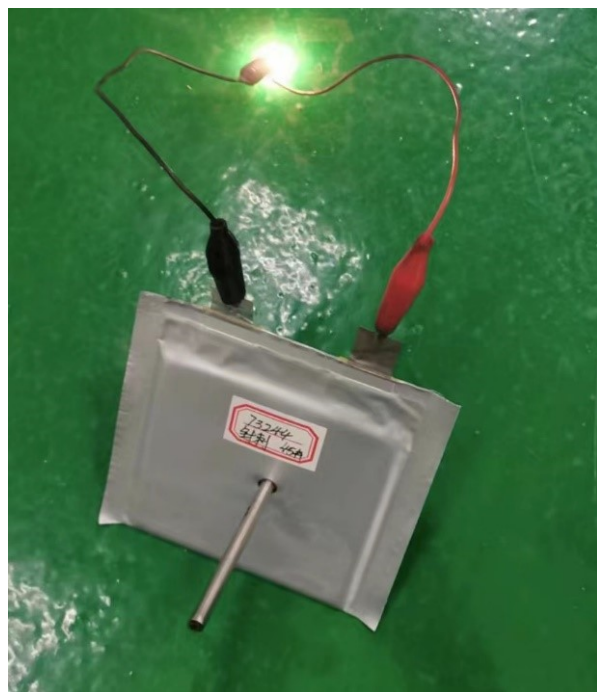


**Fig. S12.** Pinprick testing of pouch battery.

**Table. S1.** Composition of different GPEs.

	TGD (g)	TFM (g)	TCGG (g)	AIBN (mg)
0.8TGD-TCGG	0.8	0	4.5	8
0.6TGD-0.2TFM-TCGG	0.6	0.2	4.5	8
0.4TGD-0.4TFM-TCGG	0.4	0.4	4.5	8
0.2TGD-0.6TFM-TCGG	0.2	0.6	4.5	8

**Table. S2.** Ionic conductivities ( $\sigma$ ) of GPEs.

	0.8TGD-TCGG-SiO <sub>2</sub> NF (S cm <sup>-1</sup> )	0.6TGD-0.2TFM-TCGG-SiO <sub>2</sub> NF (S cm <sup>-1</sup> )	0.4TGD-0.4TFM-TCGG-SiO <sub>2</sub> NF (S cm <sup>-1</sup> )	0.2TGD-0.6TFM-TCGG-SiO <sub>2</sub> NF (S cm <sup>-1</sup> )
30 °C	1.67×10 <sup>-4</sup>	2.60×10 <sup>-4</sup>	3.56×10 <sup>-4</sup>	2.15×10 <sup>-4</sup>
40 °C	1.97×10 <sup>-4</sup>	2.74×10 <sup>-4</sup>	4.21×10 <sup>-4</sup>	2.57×10 <sup>-4</sup>
50 °C	2.35×10 <sup>-4</sup>	3.02×10 <sup>-4</sup>	4.70×10 <sup>-4</sup>	3.24×10 <sup>-4</sup>
60 °C	2.73×10 <sup>-4</sup>	3.10×10 <sup>-4</sup>	4.80×10 <sup>-4</sup>	3.58×10 <sup>-4</sup>
70 °C	3.05×10 <sup>-4</sup>	3.29×10 <sup>-4</sup>	5.00×10 <sup>-4</sup>	3.79×10 <sup>-4</sup>
80 °C	3.17×10 <sup>-4</sup>	3.53×10 <sup>-4</sup>	5.10×10 <sup>-4</sup>	4.10×10 <sup>-4</sup>

**Table. S3.** The electrochemical performances of this work and reported GPEs.

Battery	$t_{\text{Li}^+}$	Test conditions	Initial capacity (mAh g <sup>-1</sup> )	Cycles capacity retention	Reference
NCM811 TFEMA-VEC Li	0.44	3~4.5 V 25 °C	1C, 218	300 <sup>th</sup> , 70%	[1]
LFP PEGDMA-ETFP/Li	0.42	2.5~3.8 V 25 °C	0.5C, 142.1	100 <sup>th</sup> , 98%	[2]
NCA MA-HFMA-MMA Li	0.47	3~4.3 V 25 °C	0.5C, 162.2	200 <sup>th</sup> , 91%	[3]
LFP PEGDA-ETPTA Li	0.7	2.5~4.0 V 25 °C	1C, 124.4	200 <sup>th</sup> , 76%	[4]
LCO PVCA Li	0.57	2.5~4.3 V 50 °C	0.1C, 146.0	150 <sup>th</sup> , 82%	[5]
NCM811 0.4TGD-0.4TFM- TCGG-SiO <sub>2</sub> NF Li	0.57	3~4.3 V 25 °C	2C, 178.4	300 <sup>th</sup> , 92%	This work
		3~4.5 V 25 °C	2C, 184.2	260 <sup>th</sup> , 91%	

## References

- [1] Wang Y, Chen S S, Li Z Y, et al. In-situ generation of fluorinated polycarbonate copolymer solid electrolytes for high-voltage Li-metal batteries[J]. Energy Storage Materials, 2022, 45: 474-483.
- [2] Li J, Huo F, Yang Y. Constructing stable lithium interfaces via coordination of fluorinated ether and liquid crystal for room-temperature solid-state lithium metal batteries[J]. Chemical engineering journal, 2022(433P2).
- [3] Ma Y, Sun Q, Wang Z, et al. Improved interfacial chemistry and enhanced high voltage-resistance capability of an in situ polymerized electrolyte for  $\text{LiNi}_{0.8}\text{Co}_{0.15}\text{Al}_{0.05}\text{O}_2$ -Li batteries[J]. Journal of Materials Chemistry A, 2021, 9(6): 3597-3604.
- [4] Shao D, Wang X, Li X, et al. Internal in situ gel polymer electrolytes for high-performance quasi-solid-state lithium ion batteries[J]. Journal of Solid State Electrochemistry, 2019, 23(10): 2785-2792.
- [5] Chai J, Liu Z, Ma J, et al. In Situ Generation of Poly (Vinylene Carbonate) Based Solid Electrolyte with Interfacial Stability for  $\text{LiCoO}_2$  Lithium Batteries[J]. Advanced Science, 2017, 4(2).